

solution, such as the computation of weapon-delivery release time, is in progress and a malfunction results in the switching of operation to the other computer, any delay could affect overall system performance. When redundant modes remain dormant and are activated only when the primary mode is inoperable, transients caused by switching will occur in some mode mechanizations. These transients can be minimized by continuous operation of affected redundant modes. Since weapon delivery accuracy is of utmost importance, the weapon delivery equations are solved simultaneously in both F-111D computers.

There are other factors which cause the programming task and the total storage utilization to increase as a result of the use of two computers. These are:

1) Self-test. A very efficient self-test program must be implemented in order to detect failures in flight so that the switching of operation can be controlled.

2) Communication. The computers must communicate with each other; consequently, additional programming and input-output operations are required.

3) Duplication. There are certain functions, such as executive programs and mathematical subroutines, that must be duplicated in each computer.

The end result is that two computers do not provide twice the performance of one when they are operated in a dual computer configuration, such as the F-111D computer complex. Therefore, allowance for this factor must be made in the determination of individual computer performance requirements.

SEPT.-OCT. 1969

J. AIRCRAFT

VOL. 6, NO. 5

## Thunderstorm Turbulence and Its Relationship to Weather Radar Echoes

J. BURNHAM

*Royal Aircraft Establishment, Bedford, England*

AND

J. T. LEE

*National Severe Storms Laboratory, Norman, Okla.*

**Measurements of turbulence intensity made during 100 penetrations of storms in Oklahoma by instrumented aircraft, at altitudes between 23,000 ft and 37,000 ft, have been compared with properties of the weather radar echoes from the storms. The frequency of encounters with moderate and severe turbulence increased markedly with the maximum radar reflectivity of the storm. The frequency of severe turbulence encounters was greater during penetrations that passed through storm cores than during those that missed the cores by five miles or more, and somewhat greater near 25,000 than at 35,000 ft. The aeronautical implications of the study and the extrapolation of results to storms in other parts of the world are discussed.**

### 1. Introduction

THUNDERSTORMS have been a severe hazard to aircraft throughout the history of flying. The hazards of hail and turbulence in relation to flight were first documented systematically during the Thunderstorm Project of 1946-47<sup>1,2</sup>; later, United Air Lines conducted important studies in conjunction with commercial flights over midwestern United States during the 1950's.<sup>3</sup> The problem has been highlighted by accidents and incidents involving jet transports,<sup>4</sup> and it appears that flight through thunderstorms is best avoided by transport-type aircraft. The economies of civil aviation operations demand that disruption of normal services be minimized, however, while a satisfactory level of safety is maintained.

In an attempt to increase understanding of thunderstorm turbulence in relation to aircraft design and the planning of safe flight operations in a stormy atmosphere, a team of scientists from the Royal Aircraft Establishment spent six weeks during May and June 1965, in Oklahoma, working in

collaboration with scientists from the U.S. National Severe Storms Laboratory, Norman, Oklahoma. This paper reports on one aspect of this cooperative program, which has been partially documented elsewhere,<sup>5</sup> and extends other earlier studies.<sup>6-9</sup>

### 2. The Test Aircraft and Their Instrumentation

The test aircraft discussed here were an F100F of the Aeronautical Systems Division, USAFSC, Wright Patterson AFB, Dayton, Ohio, and a Seimitar F1 of the Royal Aircraft Establishment, Bedford, England. These swept-wing transonic fighters have similar dynamic characteristics at the speeds and altitudes used in the tests. Parameters recorded continuously on galvanometer oscilloscopes included the acceleration of the center of gravity normal to the aircraft axes, the airspeed, and the barometric height. The frequency response of the accelerometer channels on the two aircraft was similar and covered the rigid body and first few aeroelastic modes.

### 3. Ground-Based Radars

The primary meteorological radar was the WSR-57 of the National Severe Storms Laboratory (NSSL). This radiates a 10-cm wavelength and is equipped with both a step attenuation program and a contoured echo intensity presentation<sup>10</sup> (Fig. 1). The measure of the strength of radar echoes used

Received November 18, 1968, revision received April 3, 1969. The study reported here has been supported by the U.S. Federal Aviation Administration, NASA, and U.S. Air Force, as well as the authors' organization. The authors wish to express their appreciation for the suggestion and assistance provided by E. Kessler, Director of the National Severe Storms Laboratory, and to H. Murphy, the FAA Controller assigned to the project.

here is the radar reflectivity factor  $Z_e$ , as discussed by Battan<sup>11</sup> and by Wilk and Kulshrestha<sup>12</sup> and considered in detail in the Appendix. The radar data are based on values integrated over a 2.5-naut-mile square grid, similar to the digitized format described in Ref. 13, and were obtained with the radar beam tilted to illuminate the lower levels of the storms. Values of  $Z_e$  are quoted in units of  $\text{mm}^6/\text{m}^3$ .

Because the aircraft position was rarely shown by the WSR-57 radar, the aircraft track was obtained from a CPN-18 radar at NSSL used for aircraft control purposes. Average errors of aircraft position in relation to storms are estimated to be one or two miles, and individual errors are unlikely to exceed three miles.

#### 4. Flight Test Operations

On test days, the aircraft departed from Tinker AFB, Oklahoma, as soon as reasonably strong echoes were apparent on the WSR-57 radar at NSSL. Using the CPN-18 radar display adjacent to the WSR-57 display, an FAA controller vectored the aircraft along a track suggested by the directing scientists. On some occasions, one aircraft completed its penetrations and was succeeded by the other while the first returned to base to refuel. On others, both aircraft flew at the same time, penetrating the same storm in succession in a race track pattern.

Since the aircraft remained on the ground until storms developed, a relatively large proportion of them were sampled in mature and decaying stages. Penetrations were usually aimed at the part of a storm having the highest reflectivity. Based on earlier experience in the U.S. National Severe Storms Program, storms containing significant areas whose echo intensity ( $Z_e$ ) was  $10^5$  or more were deliberately avoided to minimize encounter with large hail.

Both aircraft were flown by qualified test pilots who maintained the attitude of the aircraft approximately constant. No flying difficulties were caused by turbulence. Both aircraft, however, suffered occasional Pitot-static system failures, with resulting loss of airspeed and height indications, because of water entering the system. In the later flights, the Scimitar was flown with the yaw damper inoperative because a potentially dangerous malfunction occurred on one flight when water entered the rudder *q*-feel system. Both aircraft also suffered occasional lightning-induced failures of the a.c. electrical system. Data from 46 storm encounters by the F100 and 54 encounters by the Scimitar are used here.

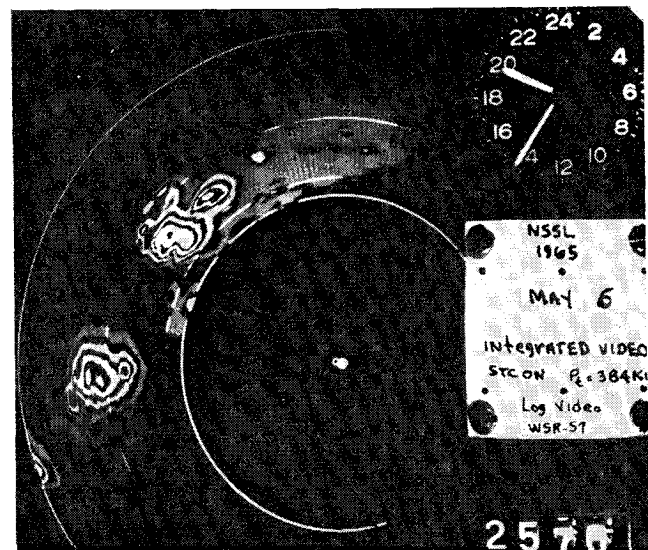


Fig. 1 Integrated log contour radar scope display of NSSL WSR-57 radar.

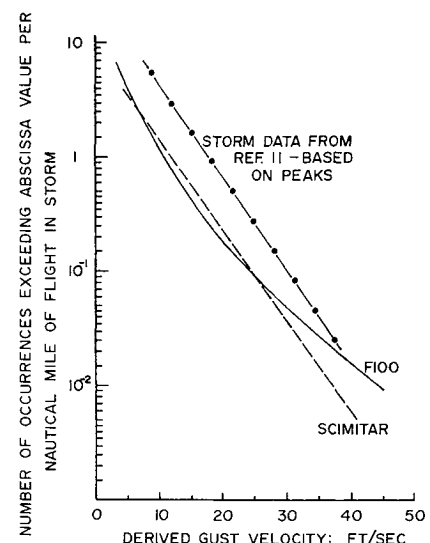


Fig. 2 Average frequencies of derived gust velocity values exceeded per naut mile for F100 and Scimitar data.

#### 5. Derived Gust Velocities as a Measure of the Severity of Turbulence

The derived gust velocity is used by aeronautical engineers to relate peak normal accelerations measured in turbulence on one type of aircraft to those which would be experienced by another aircraft flying through the same turbulence. The derived gust velocity bears no strict relationship to the actual motion of the air flown through by the measuring aircraft, but does provide a measure of the severity of the turbulence, which is independent, to the first order, of the aircraft on which it is measured. This quantity is usually denoted by  $u_{de}$  and is quoted in terms of equivalent airspeed:  $u_{de} = w_1(\rho/\rho_0)^{1/2}$ , where  $w_1$  is in ft/sec and  $\rho/\rho_0$  is the ratio of the air density at flight altitude to that at sea level in a standard atmosphere.

As a measure of the turbulence of the rough air encountered, derived gust velocities are used here mainly in two forms. The maximum derived gust velocity  $u_{de_{max}}$  corresponds to the largest incremental (relative to normal gravity) acceleration measured on a particular penetration ( $u_{de_{max}}$  being quoted as positive whether the associated peak acceleration is positive or negative). It is used as a measure of the strongest gust encountered. The root-mean-square (rms) derived gust velocity  $\sigma_{ude}$  corresponding to the rms incremental acceleration for the whole of a penetration (based on a power spectrum approach), is used as a measure of the over-all severity of the turbulence.

#### 6. Test Results

##### 6.1 Comparison of Derived Gust Velocities Measured on F100 and Scimitar Aircraft

Figure 2 shows the average frequency of encountering given values of derived gust velocities per mile of flight. The data are based on crossings of given values of incremental acceleration. Although the results defined by the two aircraft are in substantial agreement, the curve for the F100 is somewhat more bent than that for the Scimitar; this bend may be attributable to the effects of the automatic leading edge slats on the F100, which begin to open when the normal acceleration exceeds about  $1.2 g$  (total, at the test altitude and airspeed), and may give a larger value of wing-lift curve slope in the stronger gusts. The value of lift curve slope used in the calculation of derived gust velocities for the F100 is the value appropriate to the slats-closed configuration.

Data from earlier thunderstorm studies<sup>14</sup> are also shown in Fig. 2, but the data are not strictly comparable. In the earlier study peak accelerations were counted, whereas the

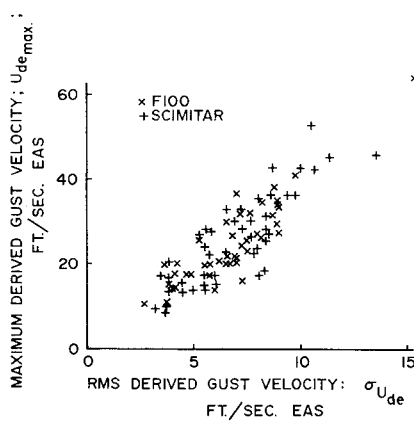


Fig. 3 Root mean square and maximum derived gust velocities encountered by F100 and Scimitar aircraft.

present results were obtained by counting crossings of acceleration levels, which number slightly less than the number of peaks. Also, during the period when the data from Ref. 14 were collected, no restriction was placed on the severity of the storms penetrated, and data from storms more intense than those penetrated in the present tests are probably included. Therefore, the difference between the present and past results in Fig. 2 is no greater than one would expect.

The maximum and rms-derived gust velocities obtained on each penetration are shown in Fig. 3, different symbols being used for the F100 and Scimitar. Results from the two air-

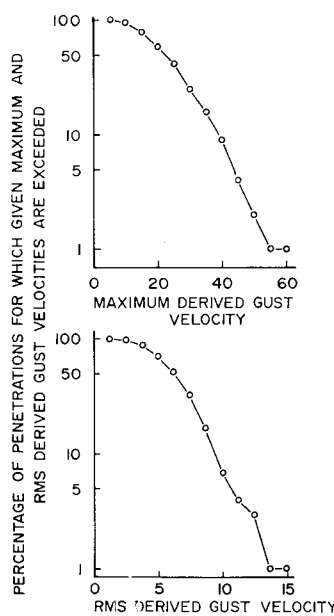


Fig. 6 Probability of encountering given maximum and rms-derived gust velocities for storms of given maximum radar reflectivity.

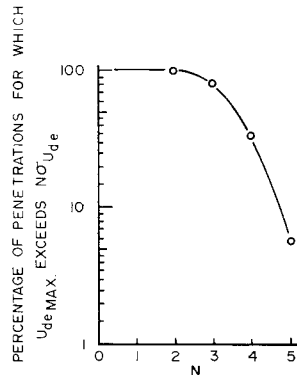


Fig. 4 Percentage of penetrations for which maximum derived gust velocity exceeds a given factor times rms-derived gust velocity.

craft are in good agreement and are combined in the remainder of the paper.

## 6.2 Relationship between Maximum and rms-Derived Gust Velocities

The percentage of penetrations for which the maximum derived gust velocity exceeds a given multiple of the rms is shown in Fig. 4. The maximum exceeds four times the rms for 33% of the storm runs and five times the rms for 5% of them. The measured frequencies of normal accelerations show that the maxima are far larger than those corresponding

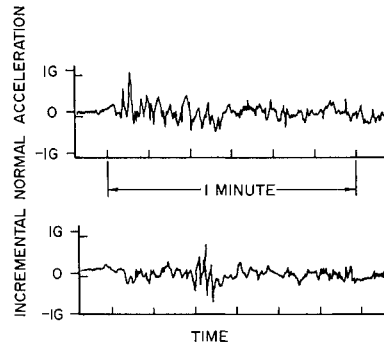


Fig. 5 Typical time histories of incremental normal accelerations measured during thunderstorm penetrations.

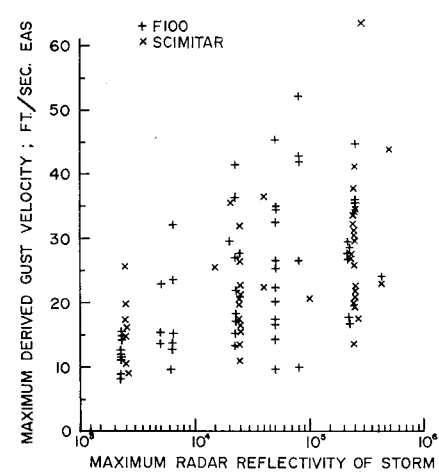


Fig. 7 Maximum derived gust velocity vs maximum radar reflectivity.

to a stationary Gaussian process. Two typical time histories are shown in Fig. 5.

The distribution of percentage of flights encountering given rms and maximum derived gust velocities is shown in Fig. 6. Maximum derived gust velocities exceeding 40 fps occurred on 9% of the penetrations and rms-derived gust velocities exceeding 10 fps occurred on 7%.

## 6.3 Relationship between Turbulence Intensity and Radar Echoes

Previous studies<sup>7-9</sup> have shown that the most severe turbulence tends to occur in storms that contain the largest radar reflectivity values ( $Z_e$ ). This is confirmed by the plot of maximum derived gust velocity against maximum radar reflectivity for storms shown in Fig. 7. The relationship becomes clearer if the radar reflectivities are stratified and derived gust velocities calculated for each group. Such results for maximum and rms-derived gust velocities are shown in Fig. 8. Note the anomalous distribution of maximum derived gust velocities for reflectivities in the ranges  $10^{4.5}$ - $10^5$  and  $10^6$ - $10^7$  with some portions of the  $10^{4.5}$  classification indicating more severe turbulence than the  $10^{5.0}$  classification. This is discussed in Sec. 6.4.

Besides maximum reflectivity, three other properties of the storm's radar echo have been considered. These are the maximum reflectivity occurring along the track of the penetrating aircraft ( $Z_{e,max}$ ), the largest gradient of reflectivity

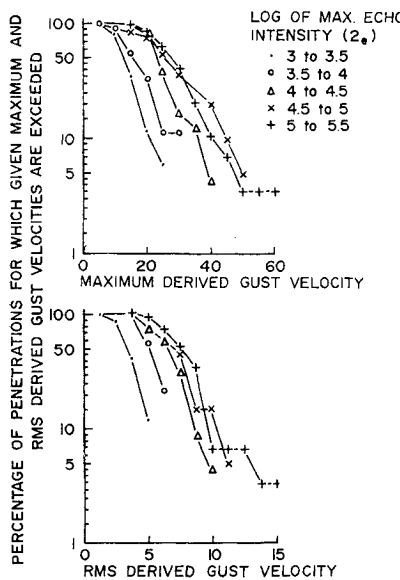


Fig. 8 Percentage of penetrations encountering given maximum and rms-derived gust velocities for storms of given maximum radar reflectivity.

$(dZ_e/dx)_{\max}$  (measured by the change in reflectivity over 2.5 naut miles), occurring along this track, and the average reflectivity gradient  $(dZ_e/dx)$  along the track. The data show that none of these quantities add appreciably to the measure of turbulence given by radar reflectivity alone.

#### 6.4 Observed Relationships between Penetration Altitude and Turbulence Intensity

The frequency of encounters with given maximum and rms-derived gust velocities in three altitude bands is shown in Fig. 9. The probability of encountering large values of derived gust velocity appears to be higher in the 23,000- to 27,000-ft band, particularly in the case of the maximum derived gust velocity. All values between 40 and 60 fps found in the tests occurred in this band. The distributions of maximum radar reflectivity for the penetrations in each of the three altitude bands are shown in Fig. 10. If higher reflectivity values were associated with higher frequencies of strong gusts, then Fig. 10 should show the least number of strong gusts in the lowest altitude band. This contrasts with the trend shown in Fig. 9. Since the storms penetrated at lower altitudes were somewhat

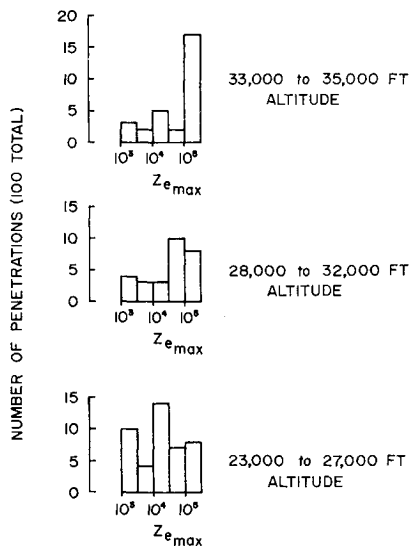
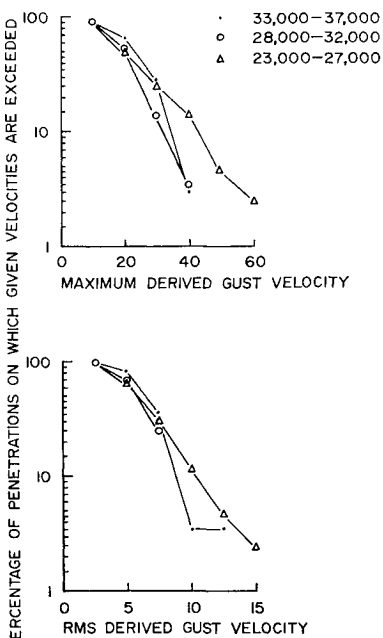


Fig. 10 Histograms of maximum radar reflectivity for storm penetrations at different altitudes.

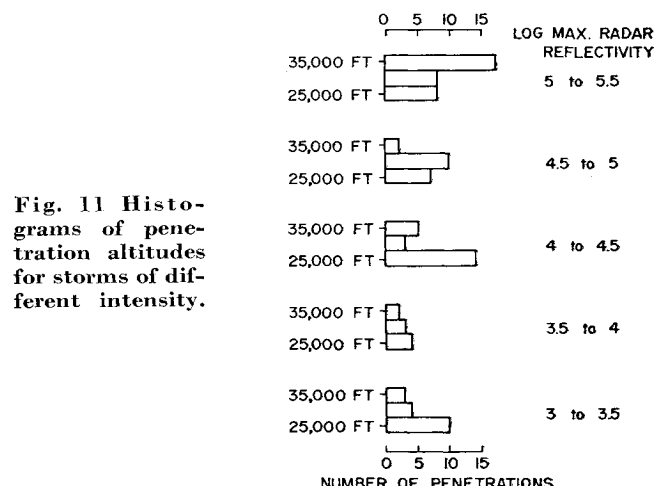
less intense on the average, the real variation of gust intensity with height may be somewhat larger than indicated in Fig. 9. Results of the Thunderstorm Project<sup>1</sup> show a tendency for the number of cases of severe turbulence to be greater around 15,000 ft, but variation of turbulence with height is not statistically significant in either study.

The possible relationship between penetration altitude and turbulence intensity may explain the anomaly shown in Fig. 8. Turbulence in storms with maximum reflectivities in the range  $10^{4.5}$  to  $10^5$  was more intense than in those in the range  $10^5$  to  $10^{5.5}$ . Perhaps this result is attributable to the distribution of penetration altitudes, as shown in Fig. 11.

#### 6.5 The Relationship between Turbulence Intensity and the Distance by Which the Penetration Missed the Storm Core

The results were examined for differences between turbulence intensity during flights which passed through the strongest radar echo and during flights which passed through a radar echo while missing the core by more than five miles. This is shown diagrammatically in Fig. 12.

Results for storm penetrations in the 23,000- to 27,000-ft altitude band with a maximum radar reflectivity greater than  $10^4$  are given in Fig. 13, which shows that more of the high values of derived gust velocity occurred on penetrations through the storm core. The actual distributions of maximum radar reflectivities for these two sets of penetrations are shown in Fig. 14. Maximum reflectivity values for the core



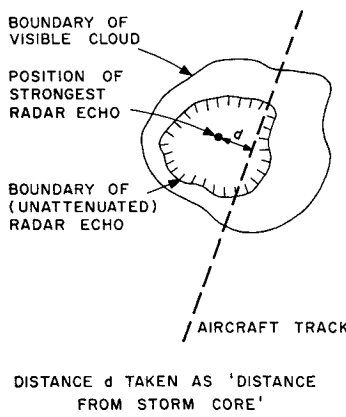


Fig. 12 Sketch showing how "distance from storm core" is defined.

penetrations were generally lower, indicating that the difference in the two sets of penetrations would be greater if the data were normalized with respect to reflectivity. Comparable results for all penetrations, irrespective of altitude, are shown in Fig. 15. Note that bias resulting not only from storm intensity but also from the effects of penetration altitude is present here. Altitude, maximum radar reflectivity, and distance from the storm core are shown in Fig. 16 for all penetrations giving a maximum derived gust velocity exceeding 30 fps.

#### 6.6 The Relationship between the Position and Intensity of the Turbulence and Radar Echoes

Time histories of the aircraft-measured quantities allowed the position and intensity of the turbulence encountered to be seen in relation to the radar echoes as shown in Fig. 17.

According to the Scimitar data and pilot reports on the F100, turbulence of more than relatively mild intensity (i.e.,  $u_{de} \geq 6$  fps) was not encountered outside visible cloud, or more than about five miles from the edge of the radar echoes. (The edge of the radar echo does not always coincide with the edge of visible cloud, which sometimes extends 5 to 10 miles outside the echo.)

Occasionally quite large gusts were encountered just inside and very close to the cloud edge. When this occurred, the

edge of the visible cloud usually appeared to coincide with the edge of the radar echo.

Although the most severe turbulence encountered on a particular penetration sometimes occurred at the same place as the strongest portion of the echo on the aircraft track (or closest to the strongest portion of echo in the storm), this was by no means always so. The most severe turbulence was sometimes found at the place where the radar echo was changing in intensity most rapidly and sometimes where there was no distinguishing local characteristic of the echo intensity distribution. Study of associations among turbulence, echo intensity and the echo gradient along the aircraft path is being continued.

Successive penetrations through the same part of the same storm often gave widely different values of both maximum and rms-derived gust velocity. Relationships between storm turbulence and radar echoes are essentially statistical rather than deterministic in character, as discussed in Ref. 7.

The measurements in Oklahoma were made at altitudes between 23,000- and 37,000-ft. These limits range from about the midheight of the cloud to just below the ambient tropopause, which may be near or well below the thunderstorm top. Few useful data are available inside thunderstorms at altitudes above the tropopause. The data gathered at low altitudes during the Thunderstorm Project<sup>1,2</sup> needs to be supplemented by turbulence data collected in storms and concurrent radar data.

#### 7. Extrapolation of Results to Other Altitudes and to Storms Occurring in Other Parts of the World

The most severe storms were excluded from the tests in order to avoid damaging encounters with hail, but storms with maximum reflectivities in the range of those studied occur in many parts of the world. Figure 18 compares the average frequency of gust velocities per mile of flight through thunderstorms in the present tests, with values obtained on flights through thunderstorms in Florida<sup>2</sup> and England, reported in Ref. 6. The agreement is close, but a number of points should be remembered in making a comparison. In neither the Florida nor the England tests were radar reflectivity measurements made of the storms penetrated. However, one would expect on general meteorological grounds (e.g., a lower probability of large hail from storms in England than in Oklahoma) that the proportion of storms with high radar reflectivities was somewhat smaller in England and Florida than in the present tests. Since it has been shown that the probability of strong turbulence increases with increasing reflectivity, it is not surprising that gusts of a given magnitude were more frequent in the Oklahoma storms. The penetrations reported in Ref. 6 covered a larger range of altitudes than the Oklahoma tests, but only relatively small effects of penetration altitude were noted. The comparison, therefore, seems valid.

Weather radar echoes show the distribution of precipitation particles; since these are produced in cloudy updrafts, the general airflow pattern in a storm should be quite closely related to the radar echo. Although the dimensions of this general airflow pattern are considerably larger than those of

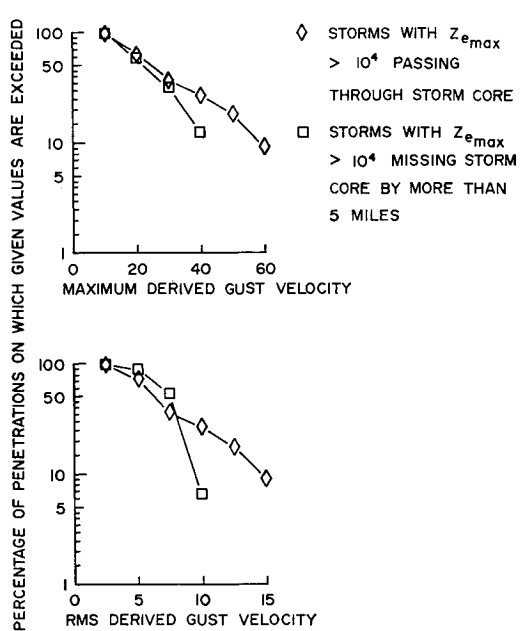


Fig. 13 Probabilities of encountering given maximum and rms-derived gust velocities for penetrations of storms, with  $Z_{e,max} 10^4$  at altitudes between 23,000 ft and 27,000 ft, showing the effect of passing through or missing the storm core.

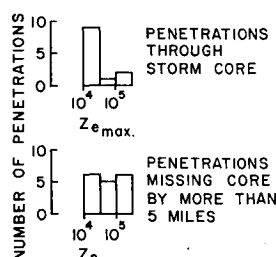


Fig. 14 Histograms of maximum radar reflectivity for penetrations at altitudes between 23,000 ft and 27,000 ft that passed through or missed the storm core.

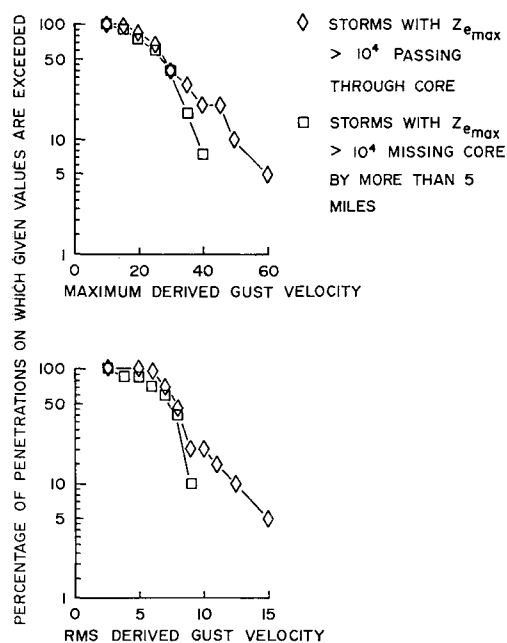


Fig. 15 Probability of encountering given maximum and rms-derived gust velocities for all penetrations of storms with  $Z_{e\max} 10^4$ , showing the effect of passing through or missing the storm core.

the turbulence considered here, one expects that increased velocities in the general pattern would correspond to increased turbulence. Such factors as atmospheric stability, water vapor, and wind affect storm development and the patterns of water and airflow. These factors may be different in Oklahoma than elsewhere, but it seems that the relationship between radar echoes and turbulence intensity should be similar.

Frequently over Oklahoma the atmospheric stratification permits excessive magnitudes of convective instability to exist for long periods until rapid overturning of the air is triggered by a suitable disturbance. In other parts of the globe where the atmosphere is either very dry or very moist throughout substantial depths, great convective instability is not present. Thus, in desert areas instability is usually quickly dissipated. In the case of large thunderstorms elsewhere, however, vertical motion and turbulence should be similar to the Oklahoma storms.

In tropical-humid climates, where the atmosphere is usually moist and slightly unstable through a great depth, strong radar

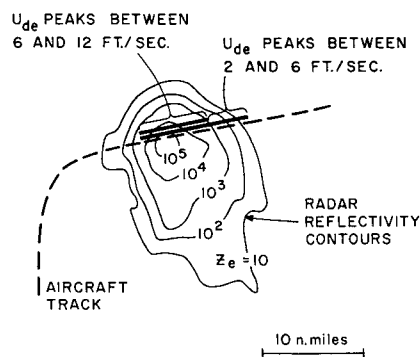


Fig. 17 Example of contours or radar reflectivity and the aircraft track, showing position and intensity of turbulence encountered.

echoes may be received from towering clouds which do not contain vertical winds as strong as those in Oklahoma. Particular occurrences are determined largely by local atmospheric conditions, and practically all geographic areas having thunderstorms occasionally report severe thunderstorms.

### 8. Aeronautical Implications of the Present Results

The results presented here are intended to provide a better appreciation of the risk involved in flight through thunderstorms and assist in the improvement of criteria used for thunderstorm avoidance. We note, however, that of the 21 cases of catastrophic structural failure of civil aircraft associated with turbulence during flights between 1945 and 1965, 17 occurred during flight in or near storms.<sup>15</sup> A reduction of turbulence accidents in thunderstorms would therefore be reflected in a very significant reduction of all turbulence accidents.

Turbulence as a direct cause of catastrophic structural failure of a civil aircraft implies derived gust velocities at least as large as about 80 fps, and probably 100 fps or more. The largest gust recorded during the Oklahoma studies was 66 fps. Not all cases of catastrophic structural failure that have occurred during flight in storm areas can be attributed directly to gust loads, however; in several cases,<sup>4</sup> the pilot lost control of the aircraft, which subsequently broke up during attempted recovery. In studying such accidents, a knowledge of true air motion is needed. Derived gust velocities do not describe adequately the long wavelength disturbances (drafts) that appear to be a main cause of control problems.

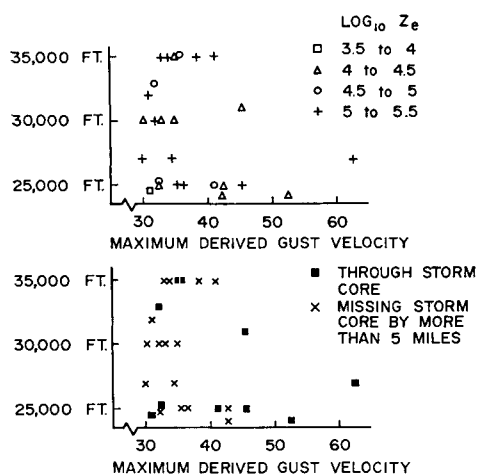


Fig. 16 Altitude, maximum radar reflectivity, and distance from storm core for all penetrations giving maximum derived gust velocities exceeding 30 fps.

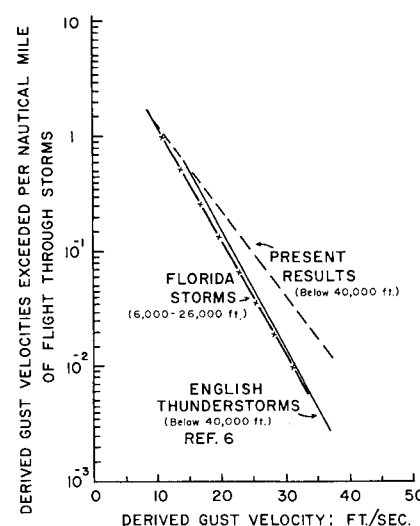


Fig. 18 Average frequencies of derived gust velocity values in thunderstorms in Florida<sup>2</sup> and in England<sup>6</sup> compared with Oklahoma results.

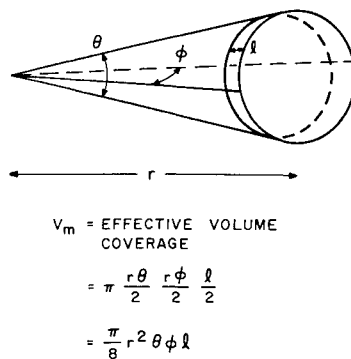


Fig. 19 Sketch illustrating derivation of effective volume coverage of radar beam.

A fairly large proportion of the injuries and occasional deaths suffered by passengers and cabin crew occur during flight through storm areas. It would be difficult to give precise values of derived gust velocities that correspond to such injuries, but values around 30 fps imply that negative  $g$  values are likely, and the probability of passenger injuries is high for values greater than this.

When relating the present results to aircraft operations, characteristics of airborne weather radar should be kept in mind. Since airborne radars are usually less sensitive than ground-based equipment and may operate at a wavelength subject to attenuation by precipitation, the echoes seen by airborne radar may be relatively small. Although airborne weather radars are sometimes equipped with a contour circuit which allows the more intense echoes to be distinguished, such radars generally do not measure the radar reflectivity accurately. Merritt<sup>16</sup> has discussed this in greater detail. Guides to the use of airborne weather radar often state that sharp reflectivity gradients, as indicated by hard echo edges and the closeness of the contours, are associated with increased probability of encountering severe turbulence.<sup>3,14</sup> Our results show that, of presently available radar parameters, the maximum reflectivity is best related to the severity of storm turbulence. The advice given in the guides is based on general experience rather than on detailed measurements. A plausible explanation of this apparent anomaly is that hard echo edges and the closeness of contours are closely related to a storm's maximum reflectivity.

During the Oklahoma tests, only relatively mild turbulence was found farther than 5 miles from the edge of unattenuated echoes or about 20 miles from the storm center shown by the WSR-57 radar. Relatively little flight time was spent between 5 and 10 miles from echo borders and cases of more severe turbulence in such areas have been reported during commercial operations. Therefore, this particular aspect of the results should be treated with considerable reserve. More quantitative information on this point and on the relationship between echo displays of ground and airborne radar is needed.

Of course, turbulence is not the only dangerous phenomenon associated with thunderstorms. Hail and large concentrations of liquid water can cause serious structural damage to aircraft; lightning is also a hazard. These hazards, the altitude range covered by the present tests, and possible reservations about the general applicability of the results to thunderstorms, also need to be kept in mind when considering ways to improve aviation safety.

## 9. Conclusions

In 1965 in Oklahoma, the U.S. National Severe Storms Laboratory and the U.K. Royal Aircraft Establishment supervised one hundred storm penetrations made by two specially instrumented aircraft at altitudes between 23,000 and 37,000 ft. Storms with maximum radar reflectivities exceeding  $5 \times 10^6 \text{ mm}^6/\text{m}^3$  were not penetrated.

The severity of turbulence encountered was similar to that found in previous studies, derived gust velocities exceeding 40

fps occurring about once per 100 miles of flight inside the storms, or once in every 10 penetrations. The turbulence was non-Gaussian in character; maximum derived gust velocities were four times the rms on 33% of penetrations. A statistical rather than deterministic relationship was found between the severity of the turbulence and the properties of the radar echoes from lower levels in the storms as seen by ground-based radar. The probability of encountering turbulence of a given intensity increases with increasing values of maximum reflectivity of the storm.

The probability of encountering severe turbulence on penetrations that pass through the core is greater than for penetrations that miss it by more than five miles. Only relatively mild turbulence was found at distances greater than 5 miles outside the edge of unattenuated echo.

It appears that the results obtained should also apply to equivalent altitudes, in storms of equal intensity, occurring in a similar air mass in other parts of the world. Further work, however, is necessary in regard to this and to the comparison of airborne and ground-based radar.

## Appendix: A Note on Radar Reflectivity

The weather radar used in the study was a WSR-57 10-cm (S band) ground-based radar with a  $1.8^\circ$  beamwidth, and a peak power output of 500 kw. The radar was used in a horizontally scanning mode to give a PPI presentation, with the antenna tilted to illuminate the lower levels of the cloud. To obtain accurate measurement of the weather echoes, a lower-range limit of 20 naut miles was used to reduce complications in the echo pattern data due to ground clutter. A 100 naut mile upper limit was used because of the large size of the illuminated volume and correspondingly poor resolution at greater distance.

The measure of radar echo intensity used here is the equivalent radar reflectivity factor  $Z_e$ . This is related to the radar measurements as follows.

The average returned power  $\bar{P}_r$  intercepted by a radar antenna looking at a target (precipitation) which fills the radar beam depends on the transmitted power  $P_t$ , wavelength  $\lambda$ , antenna gain  $G$ , range  $r$ , and the radar backscattering cross section  $\sigma$ . In the absence of attenuation,

$$\bar{P}_r = [P_t G^2 \lambda^2 / (4\pi)^3 r^4] \sigma \quad (A1)$$

as discussed by Kerr<sup>17</sup> and others. Assuming that the target consists of spherical scatterers distributed uniformly over the beam, we may express the backscattering cross section  $\sigma$  as

$$\sigma = V_m \Sigma_i \sigma_i \quad (A2)$$

where  $\sigma_i$  is the cross section of the  $i$ th particle and  $V_m$  is the volume effectively illuminated by the radar beam for one pulse length. If the radar wavelength is large compared to the dimensions of the scatterers,  $\sigma$  is given by the Rayleigh approximation to Mie Scattering theory or

$$\sigma = V_m \left[ \frac{\pi^5}{\lambda^4} |K|^2 \right] \Sigma_i D_i^6 \quad (A3)$$

where  $K$  is the dielectric factor of the target (0.9 in. for rain, 0.2 in. for snow or sleet) and  $D_i$  is the diameter of the  $i$ th particle. The quantity  $\Sigma_i D_i^6$ , the summation of the sixth powers of particle diameters in a unit volume, is the reflectivity factor designated by the symbol  $Z$ ;  $Z$  is usually expressed in  $\text{mm}^6/\text{m}^3$ . The quantity  $V_m$ , from geometrical considerations, is

$$V_m = (\pi/8) r^2 \theta \phi l \quad (A4)$$

where  $\theta$  and  $\phi$  are approximately the antenna half power beam widths in vertical and horizontal planes (see Fig. 19). Substitution of (A3) and (A4) into (A1) yields

$$\bar{P}_r = \frac{P_t \pi^3 G^2 \theta \phi l}{512 r^2 \lambda^2} |K|^2 Z \quad (A5)$$

Combining all the parameters that are essentially fixed for a given radar, such as  $\theta$ ,  $\phi$ ,  $l$ ,  $\lambda$ , and  $G$ , into a constant  $C$ , we obtain

$$\bar{P}_r = C|K|^2 Z/r^2 \quad (A6)$$

Since the actual drop size distribution is not known, the power returned is not calculated from the right side of (A7). Instead it is measured and  $Z$  is replaced by an equivalent reflectivity factor,  $Z_e$ , which is defined as the summation of a distribution (not necessarily specified) of Rayleigh scatterers that would produce the signal power actually received, or

$$Z_e = \bar{P}_r r^2 / |K|^2 C \quad (A7)$$

This quantity  $Z_e$ , which is expressed in units of  $\text{mm}^6/\text{m}^3$  as is the quantity  $Z$ , is used to compare the intensity of radar echoes.

## References

<sup>1</sup> Byers, H. R. and Braham, R. R., "The Thunderstorm," Weather Bureau, U.S. Government Printing Office, Washington, D.C., 1949.

<sup>2</sup> Press, H. and Binckley, E. T., "A Preliminary Evaluation of the Use of Ground Radar for the Avoidance of Turbulent Clouds," TN 1684, 1948, NACA.

<sup>3</sup> Beckwith, W. B., "The Use of Weather Radar in Turbojet Operation," United Air Lines Cir. No. 53, 1961, UAL, Denver, Colo.

<sup>4</sup> Bisgood, P. L. and Burnham, J., "A Review of the 'Jet Upset' Problem," R. Technical Rept. 65243, 1956, Royal Aircraft Establishment, London, England; also Rept. 27450, 1956, Aeronautical Research Council.

<sup>5</sup> Burns, A. et al., "Turbulence in Clear Air Near Thunderstorms," ESSA Tech. Memo IERTM-NSSL 30, 1966, Environmental Science Services Admin. Research Labs., Boulder, Colo.

<sup>6</sup> Jones, R. F., "The Relation between Radar Echoes from Cumulus and Cumulonimbus Clouds and the Turbulence within

those Clouds," ARC 12545, 1949, Aeronautical Research Council, London, England.

<sup>7</sup> Kessler, E., Lee, J. T., and Wilk, K. E., "Associations between Aircraft Measurements of Turbulence and Weather Radar Measurements," *Bulletin of the American Meteorological Society*, Vol. 46, No. 8, 1965, pp. 443-447.

<sup>8</sup> Lee, J. T. "Thunderstorm Turbulence and Radar Echoes; 1964 Data Studies," ESSA TN 3 and NSSL Rept. 24, 1965, Environmental Science Services Admin. Research Labs., Boulder, Colo., pp. 9-28.

<sup>9</sup> Lee, J. T., "Association between Atmospheric Turbulence and Radar Echoes in Oklahoma," ESSA Tech. Memo. IERTM-NSSL 32, 1967, ESSA Research Labs., Boulder, Colo., pp. 1-9.

<sup>10</sup> Lhermitte, R. M. and Kessler, E., "A Weather Radar Signal Integrator," NSSL Tech. Memo. 2, 1965, ESSA Research Labs., Boulder, Colo.

<sup>11</sup> Battan, L. J., *Radar Meteorology*, University of Chicago Press, Chicago, Ill., 1959, pp. 24-31.

<sup>12</sup> Wilk, K. E. and Kulshrestha S. M., "Wavelength Dependence of the Radar Reflectivity of Water and Ice Spheres," ESSA TN 3 and NSSL Rept. 24, 1965, ESSA Research Labs., Boulder, Colo., pp. 33-38.

<sup>13</sup> Kessler, E. and Russo, J. A., "Statistical Properties of Radar Echoes," *Proceedings of the 10th Weather Radar Conference*, Washington, D.C., 1963, American Meteorological Society, Boston, Mass., pp. 25-33.

<sup>14</sup> Steiner, R., "Summary of Atmospheric Turbulence Data," *NASA Conference on Aircraft Operating Problems*, 1956, NASA, Washington, D.C.

<sup>15</sup> Mitchel, C. G. B., "Some Aspects of Possible Gust Design Methods," Unpublished RAE Paper, 1967, Royal Aircraft Establishment, Farnborough, England.

<sup>16</sup> Merritt, L. P., "Preliminary Quantitative Analysis of Airborne Weather Radar," ESSA Tech. Memo. RLTM-NSSL 37, 1967, ESSA Research Labs., Boulder, Colo.

<sup>17</sup> Kerr, D. E., ed., "Propagation of Short Radio Waves," *M.I.T. Radiation Laboratory Series*, Vol. 13, 1951, McGraw-Hill, New York.